

Multi-View Adaptive Fusion Network for 3D Object Detection

Guojun Wang[†], Bin Tian[†], Yachen Zhang, Long Chen, Dongpu Cao, Jian Wu

Abstract—3D object detection based on LiDAR-camera fusion is becoming an emerging research theme for autonomous driving. However, it has been surprisingly difficult to effectively fuse both modalities without information loss and interference. To solve this issue, we propose a single-stage multi-view fusion framework that takes LiDAR Birds-Eye View, LiDAR Range View and Camera View images as inputs for 3D object detection. To effectively fuse multi-view features, we propose an Attentive Pointwise Fusion (APF) module to estimate the importance of the three sources with attention mechanisms which can achieve adaptive fusion of multi-view features in a pointwise manner. Besides, an Attentive Pointwise Weighting (APW) module is designed to help the network learn structure information and point feature importance with two extra tasks: foreground classification and center regression, and the predicted foreground probability will be used to reweight the point features. We design an end-to-end learnable network named MVAF-Net to integrate these two components. Our evaluations conducted on the KITTI 3D object detection datasets demonstrate that the proposed APF and APW module offer significant performance gain and that the proposed MVAF-Net achieves state-of-the-art performance in the KITTI benchmark.

Index Terms—3D Object Detection, Multi-View, Adaptive Fusion Network.

I. INTRODUCTION

3D object detection is particularly useful for autonomous driving applications because diverse types of dynamic objects, such as surrounding vehicles, pedestrians, and cyclists, must be identified in driving environments. Significant progress has been witnessed in the 3D object detection task with different types of sensors in the past few years, such as monocular images [1] [2], stereo cameras [3], and LiDAR point clouds [4] [5] [6]. Camera images usually contain rich features (e.g., color, texture) while suffering from the lack of depth information and affected by light and weather. LiDAR point clouds provide accurate depth and geometric structure information, which are quite helpful for obtaining 3D pose

of objects. Thus far, various 3D object detectors employing LiDAR sensors have been proposed, including PIXOR [5], VoxelNet [6], PointRCNN [7], STD [8], SECOND [9], PointPillars [10], Part-A2 [11] and CenterNet3D [12]. Although the performance of LiDAR only based 3D object detectors have been significantly improved lately, most of them operates in a single projection view, like Bird’s Eye View (BEV) or Range View (RV). BEV encoding of LiDAR points can preserve their physical dimensions and objects are naturally separable. When represented in this view, however, point clouds are sparse and have highly variable point density, which may cause detectors difficulties in detecting distant or small objects. On the other hand, RV encoding provides dense observations, which allows more favorable feature encoding for such cases. The RV representation has been shown to perform well at longer ranges where the point cloud becomes very sparse, and especially on small objects. However, no matter how to encode LiDAR returns, LiDAR point clouds are still limited for providing color and texture information. Compare with LiDAR, RGB-images from Camera View (CV) have much richer information to distinguish vehicles and background. However, they are sensitive to illumination and occlusions. Thus, the representations in different views have their own shortcomings, and only single-view input is not enough for 3D object detection for autonomous driving. This motivates us to design an effective framework to fuse features from different views for accurate 3D object detection.

In fact, a problem of fusing features from different views is challenging, especially for LiDAR points and RGB-images, as the features obtained from RGB-images and LiDAR points are represented in different perspective. When the features from RGB-images are projected into 3D LiDAR coordinates, some useful spatial information about the objects might be lost since this transformation is a one to-many mapping. And, the occlusions and illumination in RGB-images may also introduce interference information that is harmful to the object detection task. Indeed, it has been difficult for the LiDAR-camera fusion-based methods to beat the LiDAR-only methods in terms of performance. Furthermore, the large scale variations and occlusions in RV also introduce noise in feature fusion process. To solve the above issues, various LiDAR-camera fusion strategies have been proposed for 3D object detection. The previous fusion strategies can be summarized into two main categories, including 1) result-level fusion. In these methods, information aggregation happens at the result-level. The intuition behind these methods is to use off-the-shelf 2D object detectors to narrow down the region of interests for the 3D object detectors [13] [14] [15], and 2) feature-

[†]G. Wang and B. Tian contributed equally to this work.

G. Wang is with the State Key Laboratory of Automotive Simulation and Control, Jilin University, Changchun 130022, China (email: 839977837wgj@gmail.com).

B. Tian is with the State Key Laboratory of Management and Control for Complex Systems, Institute of Automation, Chinese Academy of Sciences, and with School of Artificial Intelligence, University of Chinese Academy of Sciences, Beijing 100190, China (e-mail: bin.tian@ia.ac.cn)

Y. Zhang and L. Chen are with School of Data and Computer Science, Sun Yat-Sen University, 510275, Guangzhou, China. (e-mail: zhyachen@mail2.sysu.edu.cn and chenl46@mail.sysu.edu.cn)

D. Cao is with the Waterloo Cognitive Autonomous Driving (CogDrive) Lab, University of Waterloo, Canada. (e-mail: dongpu.cao@uwaterloo.ca)

Jian Wu (Corresponding author of this paper) is a Professor of College of Automotive Engineering at Jilin University. (e-mail: wujian@jlu.edu.cn)

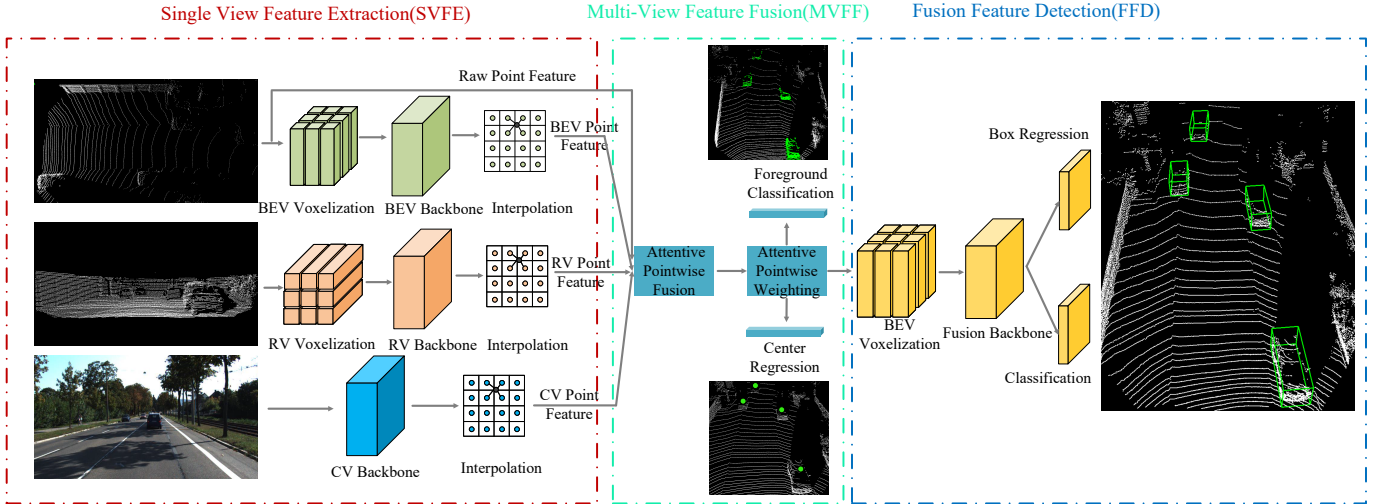


Fig. 1: Overall architecture of MVAF-Net. The overall MVAF-Net consists of three parts including the 1) Single View Feature Extraction (SVFE), 2) Multi-View Feature Fusion (MVFF) and 3) Fusion Feature Detection (FFD). In SVFE part: the raw RGB-images and point clouds are processed by three-stream CNN backbone (CV, BEV and RV backbone) to generate multi-view feature maps, where the point clouds are voxelized both in BEV and RV. In MVFF part: the multi-view features are adaptively fused with the proposed Attentive Pointwise Fusion module in a point-wise manner. The fused point features are further processed with the proposed Attentive Pointwise Weighting module to reweight the point features and learn structure information. In FFD part, the fused and reweighted point features are voxelized again and used as input of Fusion backbone for final 3D detection.

level fusion. These methods jointly reason over multi-view inputs and the intermediate features of which are deeply fused [16] [17] [18] [19] [20] [21] [22] [23]. Although effective, these methods have several limitations. Result-level fusion cannot leverage the complementarity among different views, and their performance is bounded by each stage. And, most of the previous feature-level fusion methods have been fusing features via simple concatenation or element-wise summation/mean operation, such as MV3D [16], AVOD [17], MMF [18], MVX-Net [21], PointPainting [22] and MVF [23], they do not consider the mutual interference and importance of multi-view features. However, the RGB-images from CV and range-images from RV often have noisy information such as occlusion and truncation. Thus, the wrong point features will be obtained after 3D points are projected onto the RGB-images or range images. Therefore, simply using pointwise projected features will degrade the performance of 3D detection. Recently, with the application of attention mechanisms in visual CNN models, some methods have adopted the self-attention mechanism to achieve multi-view feature fusion, such as PI-RCNN [24], 3D-CVF [25] and EPNet [26]. Although good performance has been achieved, these fusion methods generally adopt a two-stage way that uses ROI-pooling to fuse the image with the point cloud. Besides, the heavy point cloud feature extractor, such as PointNet++ [27] and 3D Convolutions (Convs) [9], further increases the computational burden of the entire network.

In this paper, to address the above challenges, we design a Multi-View Adaptive Fusion Network named MVAF-Net which can fuse the spatial feature maps separately extracted from BEV, RV and CV effectively in a point-wise manner.

It is an end-to-end single-stage LiDAR-image fusion 3D detection method without extra refinement stage, which is only composed of efficient 2D Convs. The entire network consists of three parts, namely Single View Feature Extraction (SVFE), Multi-View Feature Fusion (MVFF) and Fusion Feature Detection (FFD), as shown in Fig. 1. In SVFE part: the raw RGB-images and point clouds are processed by three-stream feature extraction network to generate multi-view feature maps, where the point clouds are voxelized into pillars in both BEV and RV. In MVFF part: the BEV, RV and CV point features are obtained by projecting the raw point clouds onto their respective feature maps and bilinear interpolation. To solve the challenges in multi-view feature fusion, we design an Attentive Pointwise Fusion (APF) module to adaptively fuse the multi-view features in a pointwise manner. Firstly, the BEV, RV and CV point features are concatenated to obtain preliminary mixed features, then the mixed point features are used as the inputs of APF module to estimate the channel-wise importance that determines how much information is brought from three sources using attention mechanisms. In this way, useful multi-view features are utilized to obtain the fused point features, while noisy features are suppressed. Comparing with previous method, our solution possesses two main advantages, including 1) achieving fine-grained pointwise correspondence between multi-view inputs through pointwise projection; 2) addressing the issue of the interference information that may be brought by CV and RV. To compensate the loss of geometric structure information of point clouds in the voxelization process, we further enrich the fused point features with raw point features.

Intuitively, points belonging to the foreground objects should contribute more to final detection tasks, while the ones

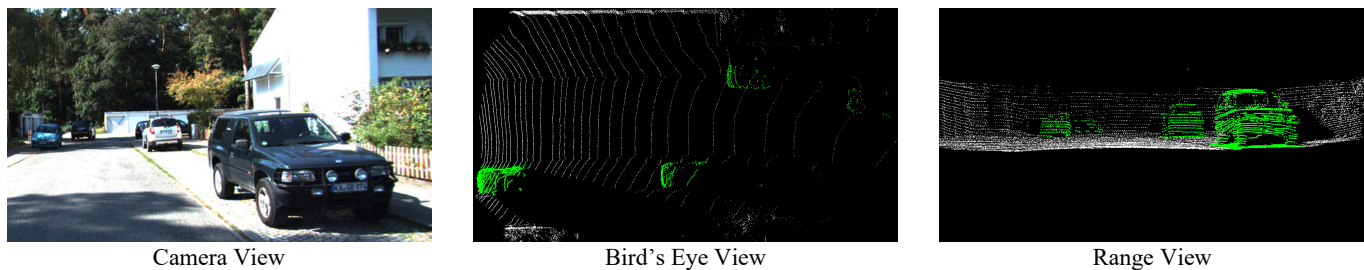


Fig. 2: Multi-view inputs of MVAF-Net.

from the background regions should contribute less. Hence, we proposed an Attentive Pointwise Weighting (APW) module to reweight the fused point features with extra supervision from foreground classification. Inspired by SA-SSD [28], we add another supervision with center regression. Thus, the APW module use the fused point features to perform two extra tasks: foreground classification to reweight the fused point features and center regression to make the features be aware of the intra-object relationship. Unlike SA-SSD, our APW module will operate during training and testing phases and is not auxiliary. And our APW module uses point features instead of voxel center features, which can better maintain geometric structure information. In FFD part, the fused and reweighted point features are voxelized again and used as inputs of Fusion Backbone for final 3D detection. The contributions of our work are summarized as follows:

- We design an Attentive Pointwise Fusion module which achieves fine-grained pointwise correspondence between multiple views through pointwise projection. The APF module can adaptively fuse features from BEV, RV and CV with attention mechanisms in a pointwise manner.
- We proposed an Attentive Pointwise Weighting module with extra supervisions from foreground classification and center regression. The predicted foreground classification can be used to reweight the fused point features and center regression can enforce CNN backbone to learn structure information and achieve better localization performance without extra cost.
- Based on Attentive Pointwise Fusion and Attentive Pointwise Weighting module, we propose a Multi-View Adaptive Fusion Network (MVAF-Net), a new 3D object fusion detection framework, that effectively combines information from multiple views: BEV, RV and CV in single stage. And it achieves state-of-the-art results on common 3D object detection benchmark KITTI datasets.

II. RELATED WORK

A. LiDAR-Only 3D Object Detection

Currently, there are four types of point cloud representations as input for 3D detectors. 1) point-based representation [7] [29]. The raw point cloud is directly processed, and bounding boxes are predicted based on each point. 2) voxel-based representation [5] [6] [9] [10] [11] [12]. The raw point clouds are converted to compact representations with 2D/3D voxelization. 3) Mixture of representations [30] [28]. In these methods,

both points and voxels are used as inputs, and their features are fused at different stages of the networks for bounding box prediction. The voxel-based methods discretize 3D point clouds into a regular feature representation, then a 2D/3D CNN backbone is applied for 3D bounding boxes prediction, such as VoxelNet [6], SECOND [9], PointPillars [10] and CenterNet3D [12]. The voxel-based methods have high computational efficiency, however the information loss is caused during the point clouds voxelization process. Point-based methods directly process raw LiDAR points using PointNet/PointNet++ [27] to yield the global feature representing the geometric structure of the entire point set, such as PointRCNN [7], STD [8] and 3DSSD [29]. Compared to the voxel-based methods, the point-based methods have flexible receptive fields for point cloud feature learning with set abstraction operation, however they are limited by the high computation cost. The methods based on mixture of representations take both points and voxels inputs and fuse their features at different stages of the networks for 3D object detection, such as PV-RCNN [30] and SA-SSD [28]. These methods can take advantages from both the voxel-based operations (i.e., 3D sparse convolution) and PointNet-based operations (i.e., set abstraction operation) to enable high computational efficiency and flexible receptive fields for improving the 3D detection performance.

B. Multi-modal Fusion based 3D Object Detection

In order to take advantages of camera and LiDAR sensors, various fusion methods have also been proposed. According to the stages of fusion occurring in the whole detection pipeline, they can be summarized into two main categories, including result-level fusion and feature-level fusion. The result-level fusion methods leverage image object detectors to generate 2D region proposals for narrowing down the region of interests for the 3D object detectors [13] [14] [15]. However, the performance of these methods is limited by the accuracy of the camera-based detectors. The feature-level fusion methods jointly reason over multi-sensor inputs and the intermediate features of which are deeply fused [16] [17] [18] [19] [20] [21] [22]. MV3D [16] is a pioneering work of this type of methods, which takes CV, RV, and BEV as input, and exploits a 3D RPN to generate 3D proposals. AVOD [17] fused the LiDAR BEV and CV features at the intermediate convolutional layer to propose 3D bounding boxes. ContFuse [19] uses continuous convolution to fuse images and LiDAR features on different resolutions. MMF [18] adds ground estimation and depth

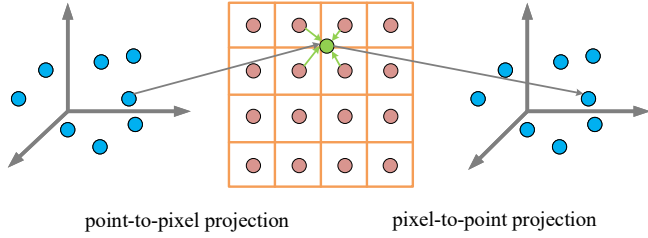


Fig. 3: Illustration of multi-view pointwise feature mapping using bilinear interpolation.

estimation to the fusion framework and learns better fusion feature representations while jointly learning multi-tasks.

While various sensor fusion networks have been proposed, they do not easily outperform LiDAR-only based detectors. Because, they have seldom paid attention to the different importance and noise of multi-view features. In the next sections, we will present our proposed MVAF-Net to overcome this challenge.

III. MULTI-VIEW ADAPTIVE FUSION NETWORK

The overall architecture of the proposed MVAF-Net is illustrated in Fig. 1. It is an end-to-end single-stage fusion 3D detection method consisting of three parts: Single View Feature Extraction (SVFE), Multi-View Feature Fusion (MVFF) and Fusion Feature Detection (FFD). In SVFE part: the raw RGB-images and point clouds are processed by three-stream CNN backbone (CV, BEV and RV backbone) to generate multi-view feature maps, where the point clouds are voxelized both in BEV and RV. In MVFF part: the multi-view features are adaptively fused with the proposed Attentive Pointwise Fusion module in a point-wise manner. The APF module can adaptively determine how much information is brought from three sources using attention mechanisms. The fused point features are further processed with the proposed Attentive Pointwise Weighting module to reweight the point features and learn structure information. In FFD part, the fused and reweighted point features are voxelized again and used as input of Fusion backbone for final 3D detection.

For simplicity in this paper, the BEV, RV, CV and Fusion backbone all use the same network architecture, but different numbers of blocks. They all have two sub-networks: one top-down network that produces features at increasingly small spatial resolution and a second network that performs upsampling and concatenation of the top-down features. The top-down backbone can be characterized by a series of convolution blocks. Each block has several 3x3 2D Conv layers followed by BatchNorm and Leaky ReLU. The first Conv layer inside each block has stride 2 to downsample the feature maps. The final features from each top-down block are upsampled to same size using transposed 2D Convs. Finally, we combine them in a concatenation manner and obtain a more representative feature map containing rich and semantic image information with different receptive fields.

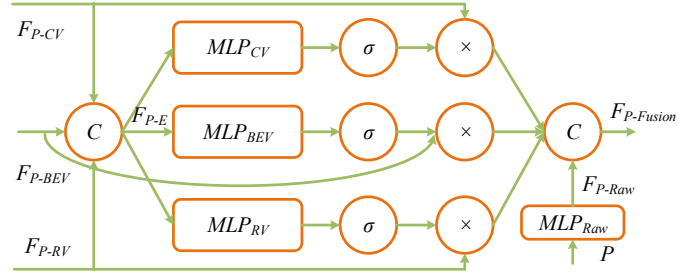


Fig. 4: Architecture of the proposed Attentive Pointwise Fusion module.

A. Single View Feature Extraction

1) *Camera View Stream*: The image stream takes RGB-images as input and extracts the semantic information with the CV backbone. The CV backbone has four blocks to downsample inputs by $16\times$, and the outputs of last three blocks are upsampled and concatenated to obtain CV feature maps F_{CV} .

2) *Bird's-Eye View Stream*: Due to the fact that BEV encoding can maintain physical dimension and scale information, as shown in Fig. 2, we voxel the point cloud into pillars in BEV. To reduce information loss and improve memory efficiency, we use dynamic voxelization to discretize the point cloud. Dynamic Voxelization is proposed by [23]. It can avoid the unstable performance caused by non-deterministic voxel embedding and unnecessary memory usage caused by voxel padding.

Specifically, dynamic voxelization in this paper consists of three steps: 1) Crop the point clouds based on the ground-truth distribution with range L, W, H m along the x, y, z axes. A point-based fully connected layer is adapted to learn high-dimensional point features. 2) The high-dimensional point features are then grouped into pillars with voxel size v_x, v_y along x, y axes and max pooling operation is employed to obtain pillar features. 3) The encoded pillar features are scattered back to the original pillar positions to construct a pseudo-image which are further processed by BEV backbone.

The BEV backbone has three blocks to downsample the pseudo-image by $8\times$, and the outputs of the three blocks are upsampled and concatenated to obtain the BEV feature maps.

3) *Range View Stream*: RV encoding is the native representation of the rotating LIDAR sensor. It retains all original information without any loss. Beyond this, the dense and compact properties make it efficient to process. Thus, we propose another Range View stream to extract point cloud features.

Like [31], we discretize the point clouds in cylindrical coordinate system. Compared with the spherical coordinate system used in [23], the cylindrical coordinate system can better maintain the scale in the z -axis direction. The cylindrical coordinates (ρ_i, ϕ_i, z_i) of a point $p_i(x_i, y_i, z_i)$ are given by the following:

$$\rho_i = \sqrt{x_i^2 + y_i^2}, \quad \phi_i = \arctan \frac{y_i}{x_i}, \quad z_i = z_i \quad (1)$$

The same dynamic voxelization operation is used for feature extraction in Range View. Firstly, a point-based fully connected layer is adapted to learn high-dimensional point features based on the cylindrical coordinates and intensity of points. The high-dimensional cylindrical point features are also grouped into pillars with voxel size v_ϕ , v_z along ϕ , z axes and max pooling operation is employed to obtain cylindrical pillar features. The encoded cylindrical pillar features are also scattered back to the original positions to construct a cylindrical pseudo-image feature map which are further processed by RV backbone. The RV backbone also has three blocks to downsample the pseudo-image $8\times$, and the outputs of the three blocks are upsampled and concatenated to obtain the RV feature maps.

B. Multi-View Feature Fusion

In MVFF part, we perform multi-view feature fusion and learning in a pointwise manner with our proposed modules: APF module and APW module. The APF module adaptively fuse multi-view features with attention mechanisms which can determine how much information is brought from three sources. The fused point features are further processed with the proposed APW module to reweight the fused point features and learn structure information.

1) *Multi-View Feature Mapping*: To fuse multi-view features in a point-wise manner, we should establish the correspondence between raw point clouds and the multi-view feature maps from the above three-stream backbone. Concretely, we project the LiDAR points onto F_{CV} , F_{RV} , F_{BEV} , using mapping matrixes M_{CV} , M_{RV} , M_{BEV} respectively. In more detail, for a particular point $p_i(x_i, y_i, z_i)$ in point cloud, we can get its corresponding position $p'_i(x'_i, y'_i)$ in the F_{CV} , which can be written as:

$$p'_i = M_{CV} * p_i \quad (2)$$

Similarly, we can get the corresponding positions in the F_{RV} and F_{BEV} . Where, M_{CV} is the LiDAR-camera-view projection matrix, M_{RV} and M_{BEV} can be obtained from the voxelization parameters in RV stream and BEV stream. Then, the multi-view point features can be obtained by bilinear interpolation on the corresponding position, as show in Fig.3.

2) *Attentive Pointwise Fusion*: To extract only essential features from multi-view point features, we propose an Attentive Pointwise Fusion module that selectively combines multi-view point features depending on the relevance to the object detection task. The proposed APF module is depicted in Fig.4. The multi-view point features F_{P-CV} , F_{P-BEV} and F_{P-RV} are concatenated channel-wise to obtain extended point features. The extended features are then fed into three channel-wise attention modules respectively, each of which uses the expanded features to adaptively estimate their respective importance in a channel-wise manner. Specifically, the expanded features are fed into their respective fully connected layers MLP_{BEV} , MLP_{CV} and MLP_{RV} , each of which includes a Linear layer, a ReLU layer, and a Linear layer. Then the respective feature weights are obtained through a sigmoid, and finally the respective attention features are obtained by multiplying the weights with the corresponding features in a

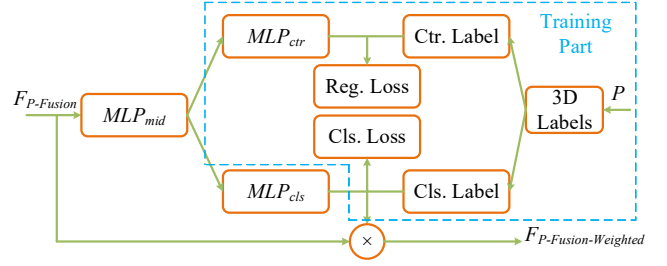


Fig. 5: Architecture of the proposed Attentive Point Weighting module.

channel-wise manner. The specific forms of channel attention are as follows:

$$\begin{cases} F_{a.P-CV} = F_{P-CV} \otimes \underbrace{\sigma(MLP_{CV}(F_{P-E}))}_{CV \text{ attention}} \\ F_{a.P-BEV} = F_{P-BEV} \otimes \underbrace{\sigma(MLP_{BEV}(F_{P-E}))}_{BEV \text{ attention}} \\ F_{a.P-RV} = F_{P-RV} \otimes \underbrace{\sigma(MLP_{RV}(F_{P-E}))}_{RV \text{ attention}} \end{cases} \quad (3)$$

where F_{P-CV} , F_{P-BEV} and F_{P-RV} represent CV, BEV and RV point features, respectively, $F_{a.P-CV}$, $F_{a.P-BEV}$ and $F_{a.P-RV}$ are the corresponding point attention features, F_{P-E} is the extended point features, σ is the sigmoid activation function and \otimes is the elementwise product operator. After obtaining the attention features, concatenate $F_{a.P-CV}$, $F_{a.P-BEV}$ and $F_{a.P-RV}$ channel-wise to get the fused point features $F_{P-Fusion}$.

We further enrich the fused point features $F_{P-Fusion}$ by concatenating the raw point features F_{P-Raw} from the raw point clouds P. In order to make the raw point features F_{P-Raw} compatible with the attention point features, a simple fully connected network called MLP_{Raw} is applied to map the raw point features to appropriate dimensions. The MLP_{Raw} is composed of a Linear layer, a BN layer, and a ReLU layer. The raw point clouds can partially make up the quantization loss of the initial pointcloud voxelization.

3) *Attentive Pointwise Weighting*: After the overall scene is encoded by the fused point features $F_{P-Fusion}$, they would be grouped into pillars again as inputs of the succeeding Fusion Feature Detection. Since the fused point feature is obtained by interpolation of multi-view 2D feature maps, which inevitably leads to the loss of 3D geometric and structural information. Besides, most of the points might only represent the background regions. Intuitively, points belonging to the foreground objects should contribute more to final object detection, while the ones from the background regions should contribute less.

Hence, we propose an Attentive Pointwise Weighting module to perform two extra tasks: foreground classification and pointwise center regression, as shown in Fig. 5. The foreground classification branch is used to predict the foreground/background probability of each point, which is further employed to reweight the fused point features. The center regression branch is used to predict the relative position of each object point to the object center. The center regression can enforce the three-stream backbone networks to learn

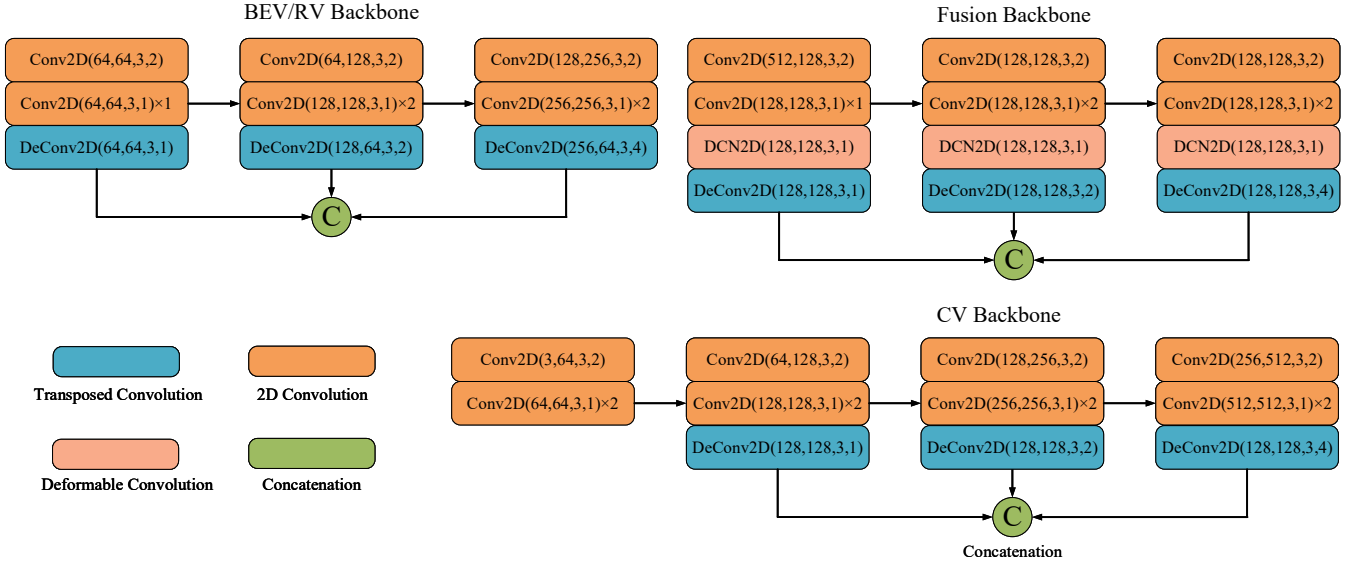


Fig. 6: The details of backbone network for MVAF-Net. Conv(cin, cout, k, s) represents a convolutional block, where cin, cout, k, s denotes input channel number, output channel number, kernel size and stride respectively. Each block consists of Convolution, BatchNorm, Leaky ReLU.

structure-aware features. The foreground classification and center regression labels can be directly generated by the 3D ground truth bounding boxes, i.e. by checking whether each point is within the 3D bounding boxes and computing the offset from the center of the bounding boxes. The two branches can be formulated as:

$$\begin{cases} F_{cls} = MLP_{cls}(MLP_{mid}(F_{P-Fusion})) \\ F_{ctr} = MLP_{ctr}(MLP_{mid}(F_{P-Fusion})) \\ F_{P-Fusion-Weighted} = F_{P-Fusion} \otimes F_{cls} \end{cases} \quad (4)$$

where, MLP_{mid} , MLP_{cls} and MLP_{ctr} are fully connected layers, MLP_{mid} includes a Linear layer, a ReLU layer, MLP_{cls} includes a Linear layer, a sigmoid layer, MLP_{ctr} only includes a Linear layer. $F_{P-Fusion-Weighted}$ is the reweighted and fused point features, \otimes is element-wise multiplication operator. The foreground classification loss L_{fore} uses focal loss, the center regression loss L_{ctr} uses SmoothL1 loss, and only the foreground points are considered for center regression loss.

C. Fusion Feature Detection

In FFD part, the fused and reweighted point features $F_{P-Fusion-Weighted}$ is again voxelized in the same way as in BEV stream to obtain pillar features. The encoded pillar features are scattered back to the original pillar positions to construct a pseudo-image. The pseudo-image features are forwarded through Fusion backbone for final 3D detection. We adopt similar detection head and loss design as [10] which comprises three parts: class classification, bounding box regression and direction classification. The class classification loss L_{cls} uses focal loss [33], bounding box regression loss L_{loc} uses SmoothL1 function to define the loss of offset from

anchor, and direction classification loss L_{dir} uses a softmax classification loss. The overall loss function can be defined as:

$$L_{total} = \beta_{loc}L_{loc} + \beta_{cls}L_{cls} + \beta_{dir}L_{dir} + \beta_{fore}L_{fore} + \beta_{ctr}L_{ctr} \quad (5)$$

IV. EXPERIMENTS

In this section, we summarize the dataset in Section A and introduce the implementation details of our proposed MVAF-Net in Section B. In Section C, we evaluate our method on the challenging 3D detection Benchmark KITTI [34]. In Section D, we present ablation studies about our method.

A. Dataset and Evaluation

We evaluate our proposed MVAF-Net on the KITTI 3D/BEV object detection benchmark. It contains the camera and LiDAR data collected using a single Pointgrey camera and Velodyne HDL-64E LiDAR. The training data contains 7,481 annotated frames for RGB image and LiDAR point cloud with 3D bounding boxes for object classes such as cars, pedestrians, and cyclists. Following the common protocol, we further divide the training data into a training set with 3,712 frames and a validation set with 3,769 frames. Additionally, KITTI provides 7,518 frames without labeling for testing. We conduct experiments on the most commonly used car category and use average precision (AP) with an (IOU) threshold 0.7 as evaluation metric. The benchmark considers three levels of difficulties: easy, moderate, and hard based on the object size, occlusion state, and truncation level. The average precision (AP) is calculated using 40 recall positions. To further compare the results with other methods on the KITTI 3D detection benchmark, we divide the KITTI training dataset into 4:1 for training and validation and report performance on the KITTI test dataset.

TABLE I: PERFORMANCE COMPARISON WITH PREVIOUS METHODS ON KITTI TEST SERVER. 3D OBJECT DETECTION METRICS ARE USED, REPORTED BY THE AVERAGE PRECISION WITH IOU THRESHOLD 0.7. THE BOLD VALUES INDICATE THE TOP PERFORMANCE.

Method	Modality	Stage	3D Detection (Car)			BEV Detection (Car)			FPS
			Easy	Moderate	Hard	Easy	Moderate	Hard	
PIXOR [5]	L	One	-	-	-	83.97	80.01	74.31	-
VoxelNet [6]	L	One	77.82	64.17	57.51	87.95	78.39	71.29	4.4
SECOND-V1.5 [9]	L	One	84.65	75.96	68.71	91.81	86.37	81.04	20
PointPillars [10]	L	One	82.58	74.31	68.99	90.07	86.56	82.81	42
PointRCNN [7]	L	Two	86.96	75.64	70.70	92.13	87.39	82.72	10
MV3D [16]	L+C	Two	74.97	63.63	54.00	86.49	79.98	72.23	2.8
F-PointNet [13]	L+C	Two	82.19	69.79	60.59	91.17	84.67	74.77	5.9
AVOD-FPN [17]	L+C	Two	83.07	71.76	65.73	90.99	84.82	79.62	10
F-ConvNet [14]	L+C	Two	87.36	76.39	66.69	91.51	85.84	76.11	2.1
MMF [18]	L+C	Two	88.40	77.43	70.22	93.67	88.21	81.99	12.5
MAFF [32]	L+C	One	85.52	75.04	67.61	90.79	87.34	77.66	24
UberATG-ContFuse [19]	L+C	One	83.68	68.78	61.67	94.07	85.35	75.88	16
MVX-Net [21]	L+C	One	85.99	75.86	70.70	91.86	86.53	81.41	6
Ours	L+C	One	85.64	77.08	70.39	91.26	88.16	83.25	15

B. Implementation Details

1) *Network Settings*: The three-stream backbone takes both the LiDAR point clouds and the RGB-images as inputs. For each 3D scene, the range of cropped LiDAR point cloud is $[-0, 70.4]$, $[-40, 40]$, $[-1, 3]$ meters along the x , y , z axes in LiDAR coordinate, respectively. A fully connected layer is used to encode raw point cloud to obtain 64-d point features in BEV and RV stream, respectively. We use a voxel size of $v_x = v_y = 0.05m$ and $v_\phi = 0.02454rad$, $v_z = 0.05m$ to group the high-dimensional point features into pillars in BEV and RV stream with dynamic voxelization, respectively. Then, max pooling operation is employed to obtain pillar features which are scattered back to the original pillar positions to construct a pseudo-image. Thus, we can get a regular feature map of size 400×352 and 80×640 in BEV and RV stream, respectively. The details of our three-stream backbone and Fusion backbone in Fig. 6, in which BEV backbone and RV backbone use the same network architecture. In order to enhance the feature learning of the network, we added deformable convolution layer to the Fusion backbone.

2) *Training Configuration*: Our entire MVAFF-Net network is end-to-end trainable and it is trained by ADAM optimizer with fixed weight decay [33] 0.01 from scratch. The learning schedule is one-cycle policy with the max learning rate set to $3e-3$, the division factor 10, the momentum range from 0.95 to 0.85. The mini-batch size is set to 2, and the model is trained for 40 epochs. In detection head, two anchors with different angles (0° , 90°) were used.

3) *Data Augmentation*: To guarantee the correct correspondence between LiDAR points and image pixels, we do not use cut-and-paste and individual ground-truth box augmentation strategy when training. This is different from most 3D detection algorithms based only based on LiDAR. We only apply random flipping, global rotation, and global scaling to the whole point cloud. The noise for global rotation is uniformly drawn from $[-\frac{\pi}{4}, \frac{\pi}{4}]$ and the scaling factor is uniformly drawn from $[0.95, 1.05]$.

C. Experimental Results on KITTI benchmark

We compare our MVAFF-Net 3D point cloud detector with other state-of-the-art approaches by submitting the detection

TABLE II: EFFECTS OF DIFFERENT FUSION SOLUTIONS ON KITTI VALIDATION SET FOR "CAR" DETECTION.

Method	3D Detection		
	Easy	Moderate	Hard
Element-wise Summation	87.53	77.56	76.29
Simple Concatenation	87.72	77.83	76.15
Attentive Pointwise Fusion	88.53	78.34	76.89

results to the KITTI server for evaluation. As shown in Table I, we evaluate our method on the 3D detection benchmark and the BEV detection benchmark of the KITTI test dataset. It can be observed that MVAFF-Net can have competitive results compared with other state-of-the-art multimodal fusion algorithms. It should be noted that MMF [18] exploits multiple auxiliary tasks (e.g., 2D detection, ground estimation, and depth completion) to boost the 3D detection performance, which requires many extra annotations. Besides, our proposed MVAFF-Net is an end-to-end single-stage fusion 3D detection method without extra refinement stage, and it shows the best performance in all single-stage fusion methods, achieving the best trade-off between speed and accuracy.

We also visualize some prediction results on the test set in Fig. 7, and we project the 3D bounding boxes from LiDAR coordinate to the RGB-images for better visualization. We can see that our approach captures the cars far away well, although these objects are usually difficult to be recognized in the RGB-images and suffer from the sparsity of the point cloud. All these challenging cases persuasively demonstrate the effectiveness of our method.

D. Ablation Studies

We conduct ablation studies to analyze the effects of the APF and APW module. All models are trained on the training set and evaluated on the validation set of KITTI dataset for Car detection. All evaluations on the validation split are performed via 40 recall positions instead of the 11 recall position.

1) *Effects of Attentive Pointwise Fusion*: We first present comparisons with two alternative fusion solutions: element-wise summation and simple concatenation in Table II. In element-wise summation (ES)/simple concatenation (SC) fusion method, we use single fully connected network to map

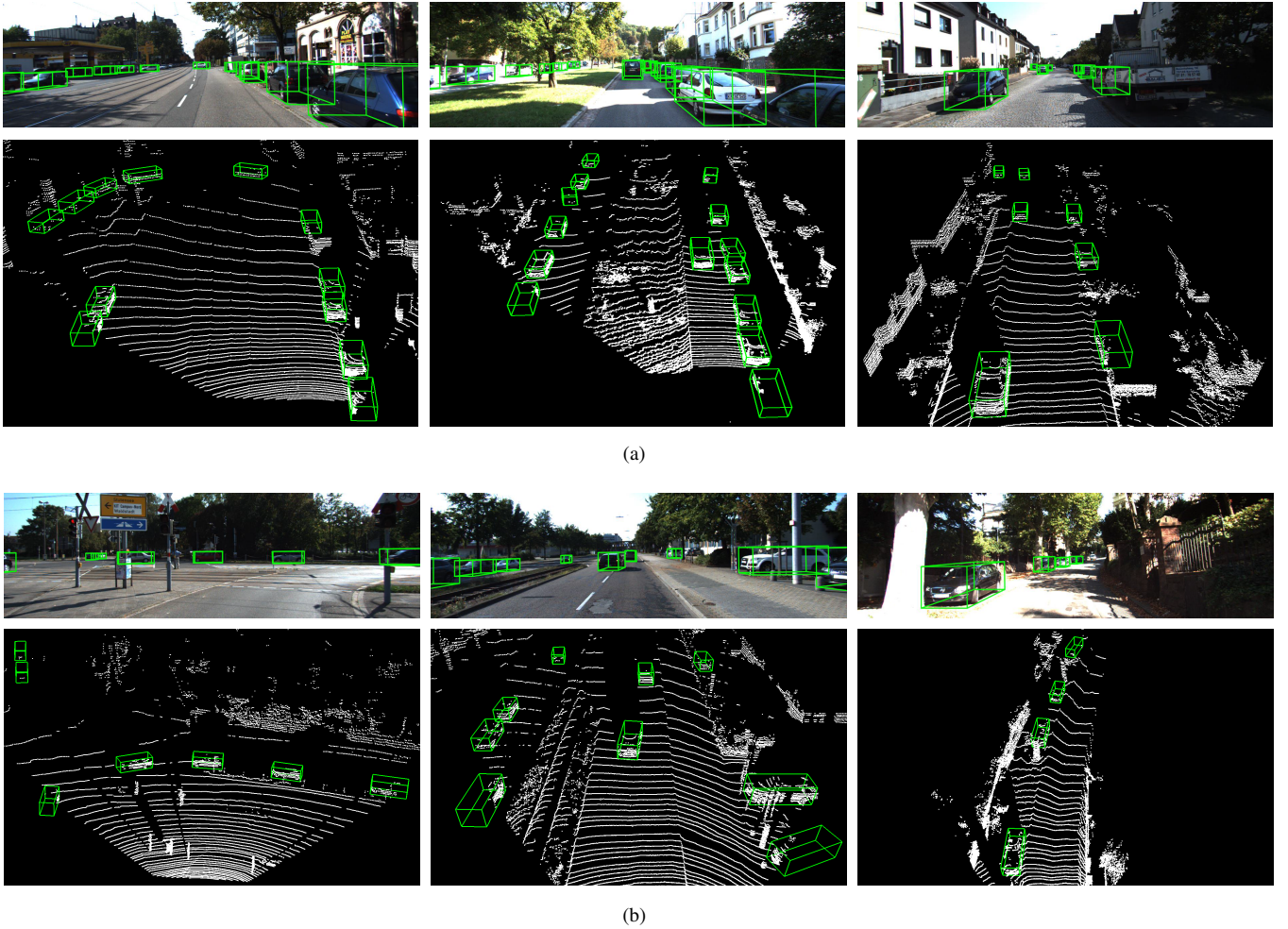


Fig. 7: Qualitative results on KITTI test set. The predicted bounding boxes are shown in green. The predictions are projected onto the RGB images (upper row) for better visualization.

the multi-view point features to the same dimension and element-wise summation/simple concatenation operation is applied to obtain fused point features. As shown in Table II, our proposed APF module yields an increment of 3D mAP 1.00%/0.78%/0.60% and 0.81%/0.51%/0.74% in Easy/Moderate/Hard level over ES and SC, respectively, which indicates that by considering channel-wise importance in multi-view features, our method can achieve better feature fusion.

To further verify the effectiveness of the proposed APF module, we investigate the importance of each component by removing point features from that view, as show in Table III. The 1st row shows that the performance drops a lot if we only aggregate features from BEV, since BEV encoding loses fine-grained information which is not enough for object detection at longer range. In 2nd and 3rd rows, the multi-view features from F_{P-RV} , F_{P-CV} contributes significantly to the performance in all three difficulty levels. The features from F_{P-RV} improves the performance 4.36%/4.55%/7.97%, especially in Hard level, which shows the advantage of RV for long-distance object detection. As shown in last four rows, the additions of raw point features F_{P-Raw} further improves

TABLE III: EFFECTS OF DIFFERENT FEATURE COMPONENTS OF APF MODULE ON KITTI VALIDATION SET FOR "CAR" DETECTION.

F_{P-BEV}	F_{P-RV}	F_{P-CV}	F_{P-Raw}	3D Detection		
				Easy	Moderate	Hard
✓				82.97	72.98	67.90
✓	✓			87.33	77.53	75.87
✓	✓	✓		87.40	77.69	76.00
✓	✓	✓	✓	88.53	78.34	76.89

the performance slightly and the best performance is achieved with all the feature components.

Besides, we also visualize the multi-view point features before APF and after APF, as shown in Fig. 8. We can see that short-distance CV point features are suppressed in first column, only distant CV point features are used. This shows that the LiDAR point features at short distances are sufficient for final 3D detection, which is in line with the fact LiDAR points are dense and informative at close distances. In second column, there are a lot of noisy features in the RV point features, especially noisy features from vegetation on both sides of the road at close distances. After the APF module, most of the noise features at close distances are suppressed.

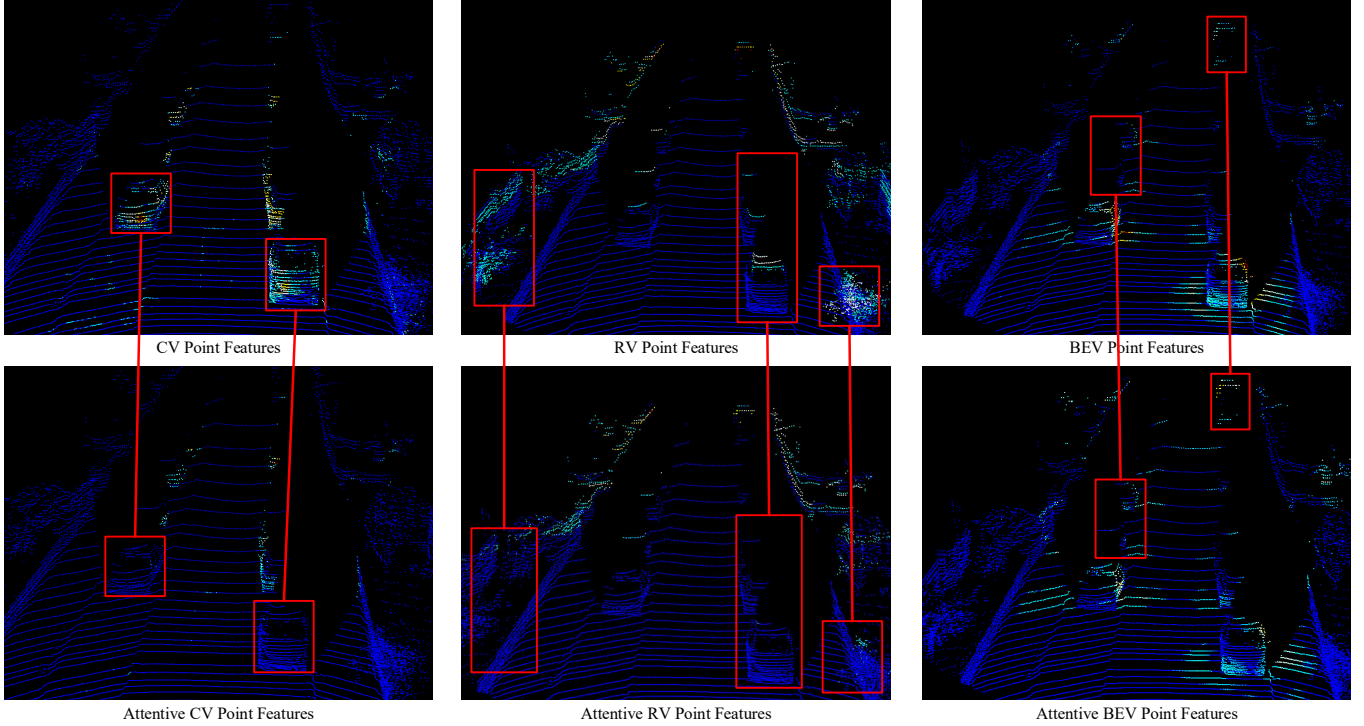


Fig. 8: Visualization of point features before/after attentive pointwise fusion module.

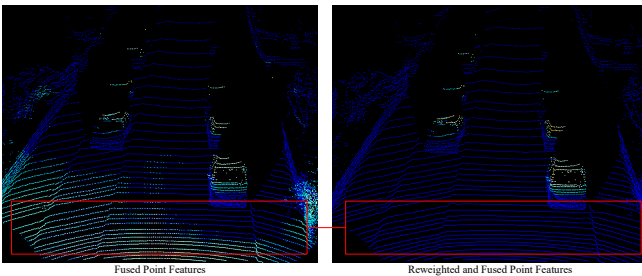


Fig. 9: Visualization of point features before/after attentive pointwise weighting module.

TABLE IV: EFFECTS OF DIFFERENT COMPONENTS OF APW MODULE ON KITTI VALIDATION SET FOR "CAR" DETECTION.

F_{cls}	F_{ctr}	$F_{weighted}$	3D Detection		
			Easy	Moderate	Hard
			86.95	77.23	75.86
✓			87.42	77.94	76.49
✓	✓		88.20	78.24	76.81
✓	✓	✓	88.53	78.34	76.89

Similarly, only the point features of the distant objects are retained, which also indicates that the BEV features at close distances are enough for final 3D detection. In third column, the BEV point features of middle and long distances are enhanced. It can be concluded that our proposed APF module can adaptively estimate the importance of multi-view point features through the attention mechanism to achieve effective multi-view feature fusion.

2) *Effects of Attentive Pointwise Weighting*: We propose the APW module to reweight the point features and learn

structure information with extra foreground classification and pointwise center regression. To prove the effectiveness of the proposed APW module, we also investigate the importance of each component of APW module on KITTI validation set. The 1st row is the MVAF-Net without APW module, we can see that the performance drops a lot which shows the effectiveness of the proposed APW module. The supervisions from F_{cls} and F_{ctr} improves the performance significantly as shown in 2nd to 3rd rows. As shown in last 4th rows, the use of foreground classification to reweight point features further improves the performance slightly and the best performance is achieved with all the components. Thus, we can conclude that the proposed APW module enables better feature aggregation by focusing more on the foreground points and learning structure information.

Besides, we also visualize the fused point features before APW and APW using point feature reweight, as shown in Fig. 9. We can see that after the APW module, most of the background point features are suppressed, which shows that our proposed APW is effective.

V. CONCLUSION

We have presented an end-to-end single-stage multi-view fusion 3D detection method, MVAF-Net, which consists of three parts: Single View Feature Extraction (SVFE), Multi-view Feature Fusion (MVFF) and Fusion Feature Detection (FFD). In SVFE part: three-stream CNN backbone (CV, BEV and RV backbone) consumes LiDAR point clouds and RGB-images to generate multi-view feature maps. In MVFF part: the adaptive fusion of multi-view features is realized using

our proposed APF module which can adaptively determine how much information is brought from multi-view inputs using attention mechanisms. Besides, we have further improved the performance of the network with the proposed Attentive Point Weighting Module which can reweight the point features and learn structure information with two extra tasks: foreground classification and center regression. Extensive experiments have validated the effectiveness of the proposed APF and APW module. Furthermore, the proposed MVAF-Net yields competitive results and it achieves the best performance in all single-stage fusion methods, achieving the best trade-off between speed and accuracy in the KITTI benchmark.

REFERENCES

- [1] X. Chen, K. Kundu, Z. Zhang, H. Ma, S. Fidler, and R. Urtasun, "Monocular 3d object detection for autonomous driving," in *Proceedings of the IEEE Conference on Computer Vision and Pattern Recognition*, 2016, pp. 2147–2156.
- [2] B. Xu and Z. Chen, "Multi-level fusion based 3d object detection from monocular images," in *Proceedings of the IEEE conference on computer vision and pattern recognition*, 2018, pp. 2345–2353.
- [3] X. Chen, K. Kundu, Y. Zhu, H. Ma, S. Fidler, and R. Urtasun, "3d object proposals using stereo imagery for accurate object class detection," *IEEE transactions on pattern analysis and machine intelligence*, vol. 40, no. 5, pp. 1259–1272, 2017.
- [4] W. Luo, B. Yang, and R. Urtasun, "Fast and furious: Real time end-to-end 3d detection, tracking and motion forecasting with a single convolutional net," in *Proceedings of the IEEE conference on Computer Vision and Pattern Recognition*, 2018, pp. 3569–3577.
- [5] B. Yang, W. Luo, and R. Urtasun, "Pixor: Real-time 3d object detection from point clouds," in *Proceedings of the IEEE conference on Computer Vision and Pattern Recognition*, 2018, pp. 7652–7660.
- [6] Y. Zhou and O. Tuzel, "Voxelnet: End-to-end learning for point cloud based 3d object detection," in *Proceedings of the IEEE Conference on Computer Vision and Pattern Recognition*, 2018, pp. 4490–4499.
- [7] S. Shi, X. Wang, and H. Li, "Pointnet: 3d object proposal generation and detection from point cloud," in *Proceedings of the IEEE Conference on Computer Vision and Pattern Recognition*, 2019, pp. 770–779.
- [8] Z. Yang, Y. Sun, S. Liu, X. Shen, and J. Jia, "Std: Sparse-to-dense 3d object detector for point cloud," in *Proceedings of the IEEE International Conference on Computer Vision*, 2019, pp. 1951–1960.
- [9] Y. Yan, Y. Mao, and B. Li, "Second: Sparsely embedded convolutional detection," *Sensors*, vol. 18, no. 10, p. 3337, 2018.
- [10] A. H. Lang, S. Vora, H. Caesar, L. Zhou, J. Yang, and O. Beijbom, "Pointpillars: Fast encoders for object detection from point clouds," in *Proceedings of the IEEE Conference on Computer Vision and Pattern Recognition*, 2019, pp. 12 697–12 705.
- [11] S. Shi, Z. Wang, J. Shi, X. Wang, and H. Li, "From points to parts: 3d object detection from point cloud with part-aware and part-aggregation network," *IEEE Transactions on Pattern Analysis and Machine Intelligence*, 2020.
- [12] G. Wang, B. Tian, Y. Ai, T. Xu, L. Chen, and D. Cao, "Centernet3d: An anchor free object detector for autonomous driving," *arXiv preprint arXiv:2007.07214*, 2020.
- [13] C. R. Qi, W. Liu, C. Wu, H. Su, and L. J. Guibas, "Frustum pointnets for 3d object detection from rgb-d data," in *Proceedings of the IEEE conference on computer vision and pattern recognition*, 2018, pp. 918–927.
- [14] Z. Wang and K. Jia, "Frustum convnet: Sliding frustums to aggregate local point-wise features for amodal 3d object detection," *arXiv preprint arXiv:1903.01864*, 2019.
- [15] D. Xu, D. Anguelov, and A. Jain, "Pointfusion: Deep sensor fusion for 3d bounding box estimation," in *Proceedings of the IEEE Conference on Computer Vision and Pattern Recognition*, 2018, pp. 244–253.
- [16] X. Chen, H. Ma, J. Wan, B. Li, and T. Xia, "Multi-view 3d object detection network for autonomous driving," in *Proceedings of the IEEE Conference on Computer Vision and Pattern Recognition*, 2017, pp. 1907–1915.
- [17] J. Ku, M. Mozifian, J. Lee, A. Harakeh, and S. L. Waslander, "Joint 3d proposal generation and object detection from view aggregation," in *2018 IEEE/RSJ International Conference on Intelligent Robots and Systems (IROS)*. IEEE, 2018, pp. 1–8.
- [18] M. Liang, B. Yang, Y. Chen, R. Hu, and R. Urtasun, "Multi-task multi-sensor fusion for 3d object detection," in *Proceedings of the IEEE Conference on Computer Vision and Pattern Recognition*, 2019, pp. 7345–7353.
- [19] M. Liang, B. Yang, S. Wang, and R. Urtasun, "Deep continuous fusion for multi-sensor 3d object detection," in *Proceedings of the European Conference on Computer Vision (ECCV)*, 2018, pp. 641–656.
- [20] M. Zhu, C. Ma, P. Ji, and X. Yang, "Cross-modality 3d object detection," *arXiv preprint arXiv:2008.10436*, 2020.
- [21] V. A. Sindagi, Y. Zhou, and O. Tuzel, "Mvx-net: Multimodal voxelnet for 3d object detection," in *2019 International Conference on Robotics and Automation (ICRA)*. IEEE, 2019, pp. 7276–7282.
- [22] S. Vora, A. H. Lang, B. Helou, and O. Beijbom, "Pointpainting: Sequential fusion for 3d object detection," in *Proceedings of the IEEE/CVF Conference on Computer Vision and Pattern Recognition*, 2020, pp. 4604–4612.
- [23] Y. Zhou, P. Sun, Y. Zhang, D. Anguelov, J. Gao, T. Ouyang, J. Guo, V. Ngiam, and V. Vasudevan, "End-to-end multi-view fusion for 3d object detection in lidar point clouds," in *Conference on Robot Learning*, 2020, pp. 923–932.
- [24] L. Xie, C. Xiang, Z. Yu, G. Xu, Z. Yang, D. Cai, and X. He, "Pi-rcnn: An efficient multi-sensor 3d object detector with point-based attentive cont-conv fusion module," in *AAAI*, 2020, pp. 12 460–12 467.
- [25] J. H. Yoo, Y. Kim, J. S. Kim, and J. W. Choi, "3d-cvf: Generating joint camera and lidar features using cross-view spatial feature fusion for 3d object detection," *arXiv preprint arXiv:2004.12636*, 2020.
- [26] T. Huang, Z. Liu, X. Chen, and X. Bai, "Epnnet: Enhancing point features with image semantics for 3d object detection," *arXiv preprint arXiv:2007.08856*, 2020.
- [27] C. R. Qi, L. Yi, H. Su, and L. J. Guibas, "Pointnet++: Deep hierarchical feature learning on point sets in a metric space," in *Advances in neural information processing systems*, 2017, pp. 5099–5108.
- [28] C. He, H. Zeng, J. Huang, X.-S. Hua, and L. Zhang, "Structure aware single-stage 3d object detection from point cloud," in *Proceedings of the IEEE/CVF Conference on Computer Vision and Pattern Recognition*, 2020, pp. 11 873–11 882.
- [29] Z. Yang, Y. Sun, S. Liu, and J. Jia, "3dssd: Point-based 3d single stage object detector," in *Proceedings of the IEEE/CVF Conference on Computer Vision and Pattern Recognition*, 2020, pp. 11 040–11 048.
- [30] S. Shi, C. Guo, L. Jiang, Z. Wang, J. Shi, X. Wang, and H. Li, "Pv-rcnn: Point-voxel feature set abstraction for 3d object detection," in *Proceedings of the IEEE/CVF Conference on Computer Vision and Pattern Recognition*, 2020, pp. 10 529–10 538.
- [31] Y. Wang, A. Fathi, A. Kundu, D. Ross, C. Pantofaru, T. Funkhouser, and J. Solomon, "Pillar-based object detection for autonomous driving," *arXiv preprint arXiv:2007.10323*, 2020.
- [32] Z. Zhang, M. Zhang, Z. Liang, X. Zhao, M. Yang, W. Tan, and S. Pu, "Maff-net: Filter false positive for 3d vehicle detection with multi-modal adaptive feature fusion," *arXiv preprint arXiv:2009.10945*, 2020.
- [33] I. Loshchilov and F. Hutter, "Fixing weight decay regularization in adam," 2018.
- [34] A. Geiger, P. Lenz, C. Stiller, and R. Urtasun, "Vision meets robotics: The kitti dataset," *The International Journal of Robotics Research*, vol. 32, no. 11, pp. 1231–1237, 2013.



GuoJun Wang received the B.S. degree in vehicle engineering from Yanshan University, Qinhuangdao, China, in 2014. He is currently pursuing the Ph.D. degree in vehicle engineering with Jilin University, Changchun, China. His current research interest includes environment perception, behavior estimation and prediction.



Bin Tian is with the State Key Laboratory of Management and Control for Complex Systems, Institute of Automation, Chinese Academy of Sciences, Beijing 100190, China, and also with the Cloud Computing Center, Chinese Academy of Sciences, Dongguan 523808, China (e-mail: bin.tian@ia.ac.cn). Bin Tian received the B.S. degree from Shandong University, Jinan, China, in 2009 and the Ph.D. degree from the Institute of Automation, Chinese Academy of Sciences, Beijing, China, in 2014. He is currently an Associate Professor of the State Key Laboratory of Management and Control for Complex Systems, Institute of Automation, Chinese Academy of Sciences. His current research interests include computer vision, machine learning, and automated driving.



Dongpu Cao received the Ph.D. degree from Concordia University, Canada, in 2008. He is a Canada Research Chair in Driver Cognition and Automated Driving, and currently an Associate Professor and Director of Waterloo Cognitive Autonomous Driving (CogDrive) Lab at University of Waterloo, Canada. His current research focuses on driver cognition, automated driving and cognitive autonomous driving. He has contributed more than 180 publications, 2 books and 1 patent. He received the SAE Arch T. Colwell Merit Award in 2012, and three Best Paper Awards from the ASME and IEEE conferences. Dr. Cao serves as an Associate Editor for IEEE TRANSACTIONS ON VEHICULAR TECHNOLOGY, IEEE TRANSACTIONS ON INTELLIGENT TRANSPORTATION SYSTEMS, IEEE/ASME TRANSACTIONS ON MECHATRONICS, IEEE TRANSACTIONS ON INDUSTRIAL ELECTRONICS and ASME JOURNAL OF DYNAMIC SYSTEMS, MEASUREMENT AND CONTROL. He was a Guest Editor for VEHICLE SYSTEM DYNAMICS and IEEE TRANSACTIONS ON SMC: SYSTEMS. He serves on the SAE Vehicle Dynamics Standards Committee and acts as the Co-Chair of IEEE ITSS Technical Committee on Cooperative Driving.



Yachen Zhang received the B.S degree from Sun Yat-Sen University, Guangzhou, China, in 2018. He is currently working toward the M.S. degree in the school of Data and Computer Science, Sun Yat-sen University, China. His research interests are in the areas of SLAM and 3D LIDAR. He is now a student under the instruction of Long Chen. He is recently focusing on cooperative mapping based on 3D LIDAR.



Long Chen received the B.Sc. degree in communication engineering and the Ph.D. degree in signal and information processing from Wuhan University, Wuhan, China. He is currently an Associate Professor with School of Data and Computer Science, Sun Yat-sen University, Guangzhou, China. His areas of interest include autonomous driving, robotics, artificial intelligence where he has contributed more than 70 publications. He serves as an Associate Editor for IEEE Transactions on Intelligent Transportation Systems.



Jian Wu is a Professor of College of Automotive Engineering at Jilin University. His research interests are mainly in vehicle control system, electric vehicles, and intelligent vehicles. He is the authors of over 40 peer-reviewed papers in international journals and conferences, and has been in charge of numerous projects funded by national government and institutional organizations on vehicles.